

Beauty production in small systems with ALICE at the LHC

Katharina Demmich¹

*Westfälische Wilhelms-Universität Münster,
Wilhelm-Klemm-Straße 9, Münster, Germany*

E-mail: katharina.demmich@uni-muenster.de

The measurement of beauty production in proton-proton (pp) collisions offers the possibility to test predictions based on perturbative Quantum Chromodynamics (QCD) calculations, to investigate mechanisms of heavy-flavour fragmentation, and to provide a reference for corresponding measurements in heavy-ion collisions. Thanks to the excellent tracking capabilities, measurements with the ALICE experiment can assess beauty production down to low momenta. In this document, recent measurements of the ALICE Collaboration on beauty production in pp collisions at $\sqrt{s} = 13$ TeV are presented.

*41st International Conference on High Energy physics - ICHEP2022
6-13 July, 2022
Bologna, Italy*

¹For the ALICE Collaboration

1. Introduction

The investigation of beauty-quark production in high-energy proton-proton (pp) collisions is motivated by several aspects. By measuring the beauty production cross section, predictions based on perturbative Quantum Chromodynamics (pQCD) calculations can be tested [1–3]. In addition, the measurement of the relative abundances of different b-hadron species allows to study the mechanisms of heavy-quark fragmentation [1]. Finally, studies on beauty production in pp collisions serve as a reference for corresponding measurements in heavy-ion collisions. Beauty quarks are effective tools to probe the properties of the Quark-Gluon Plasma [3] created in ultra-relativistic heavy-ion collisions. Moreover, non-prompt D mesons constitute the major source of background for the measurement of the spin alignment of prompt vector D mesons, which carries information about the magnetic field and the angular momentum in the initial stage of a heavy-ion collision [4].

The weak decays of b-hadrons occur with long lifetimes of $\tau \approx 450 \mu\text{m}/c$ [5]. Consequently, beauty-hadron decays produce a secondary vertex that is well displaced from the primary vertex of the collision. This property can be exploited to identify beauty-hadron decay tracks by their large displacement from the primary vertex. Within the ALICE Collaboration, lifetime-based observables are utilised for the identification of beauty in several ways. Statistical methods are applied for which the relative contribution of beauty signals is determined by template fits [2]. Further analysis methods entail the event-based identification of b-jets (“b-jet tagging”) [3] and the machine-learning (ML) based selection of non-prompt charm hadrons [1]. Due to the unique tracking performance of the Time Projection Chamber (TPC) and the Inner Tracking System (ITS), the ALICE experiment [6] offers excellent capabilities to measure beauty production down to low momenta. In these proceedings, an overview is given on recent ALICE measurements of beauty production in pp collisions at $\sqrt{s} = 13 \text{ TeV}$.

2. Results

The cross section for the production of electrons from beauty-hadron decays (“beauty electrons”) has been measured using a statistical approach. Template fits to distributions of the transverse impact parameter of tracks identified as electrons have been utilised to determine the relative abundance of beauty electrons in different transverse momentum (p_T) intervals. The ratio of the beauty-electron cross section measured in pp collisions at $\sqrt{s} = 13 \text{ TeV}$ with respect to results at $\sqrt{s} = 7 \text{ TeV}$ [7], 5.02 TeV , and 2.76 TeV [8] are shown in Fig. 1. The data are compatible with FONLL predictions [9] based on pQCD calculations with fixed-order and next-to-leading log accuracy. In addition, it was found that beauty electrons are the dominant contribution to heavy-flavour electrons for a transverse momentum of $p_T > 5 \text{ GeV}/c$.

The cross section of charged-particle b-jets has been measured as a function of the jet transverse momentum ($p_{T,\text{ch jet}}$). Jets with a radius of $R = 0.4$ have been identified with the anti- k_T algorithm and b jets have been selected based on jet constituents with a large transverse impact-parameter significance. As it can be seen in Fig. 2, the corresponding cross section measured in pp collisions at $\sqrt{s} = 13 \text{ TeV}$ is larger than the one measured at 5.02 TeV by a factor of two to six from low to large $p_{T,\text{ch jet}}$. The relative abundance of b jets to inclusive jets is compatible at the two collision energies.

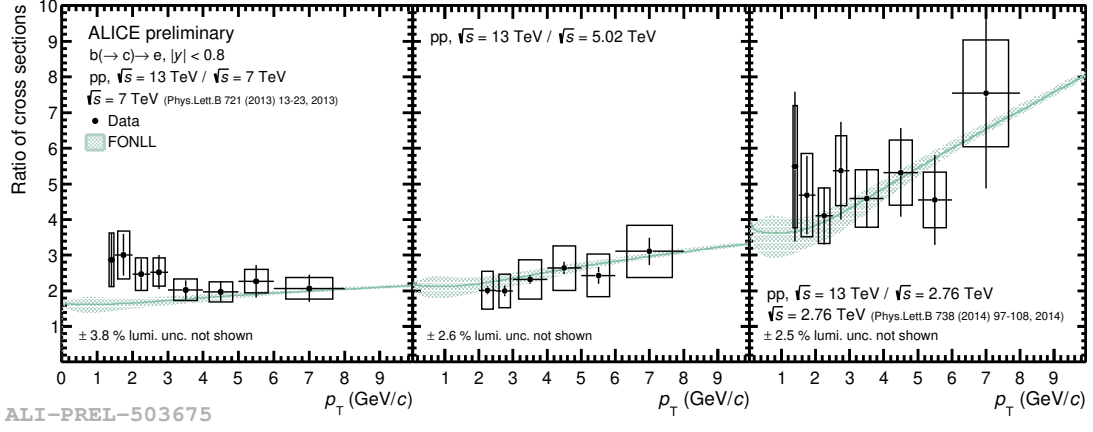


Figure 1: The ratio of the beauty-electron cross section for pp collisions at $\sqrt{s} = 13$ TeV to the corresponding cross sections at 7 TeV [7] (left), 5.02 TeV (middle) and 2.76 TeV [8] (right) as a function of p_T compared to FONLL calculations [9].

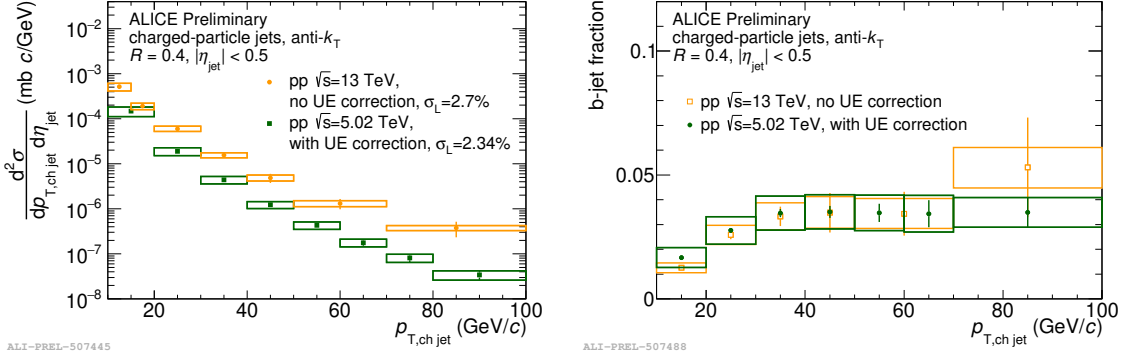


Figure 2: Comparison of charged-particle b-jet measurements for pp collisions at $\sqrt{s} = 5.02$ TeV [3] and 13 TeV. The measurement at 5.02 TeV is corrected for the underlying event (UE) contribution to the jet momentum differently from the measurement at 13 TeV. Left: the b-jet cross section as a function of $p_{T, \text{ch jet}}$. The additional normalisation uncertainties σ_L [15, 16] are quoted in the legend. Right: the b-jet to inclusive-jet p_T -differential cross-section ratio with the cross section of inclusive jet production at $\sqrt{s} = 13$ TeV from Ref. [17].

In comparison to the measurement at 5.02 TeV, the systematic uncertainties of the spectrum at 13 TeV are smaller at low $p_{T, \text{ch jet}}$.

The first measurement of the fractions $f_{\text{non-prompt}}$ of non-prompt with respect to inclusive D^0 and D^+ mesons as a function of the charged-particle multiplicity has been performed in pp collisions at $\sqrt{s} = 13$ TeV with the help of ML-based selections. The ratio of $f_{\text{non-prompt}}$ for different multiplicity ranges to the minimum-bias value is shown as a function of multiplicity ($dN_{\text{ch}}/d\eta$) in Fig. 3 (left). It exhibits a trend which, within uncertainties, is flat around unity, suggesting that $f_{\text{non-prompt}}$ does not vary significantly with the multiplicity. The data are described by predictions of a Colour Glass Condensate (CGC) parametrisation [10] as well as different tunes [11–13] of the Monte Carlo event generator PYTHIA 8 [11–13]. However, predictions for the p_T -differential ratio of the fraction of non-prompt D mesons in high-multiplicity collisions to the one in minimum-bias collisions for the

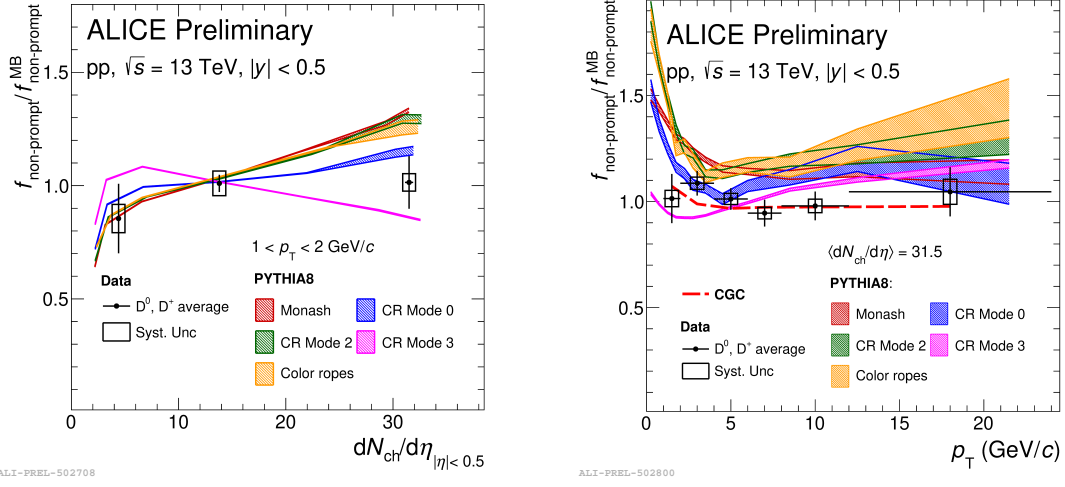


Figure 3: The ratio of $f_{\text{non-prompt}}$ for different multiplicity ranges to the minimum-bias value for pp collisions at $\sqrt{s} = 13$ TeV. The data are compared to predictions of different PYTHIA tunes [11–13]. Left: $f_{\text{non-prompt}}$ ratio as a function of the charged-particle multiplicity $(dN_{\text{ch}}/d\eta)_{|\eta| < 0.5}$ for low transverse momenta ($1 < p_T < 2$ GeV/c). Right: $f_{\text{non-prompt}}$ ratio at high multiplicities, $\langle dN_{\text{ch}}/d\eta \rangle = 31.5$, as a function of p_T .

PYTHIA tunes Monash [11], CR Mode 2 [12] and Colour ropes [13] are in tension with the data (see Fig. 3, right panel).

The p_T -differential cross section for the production of non-prompt Λ_c^+ baryons is presented in Fig. 4 (left). The Λ_c^+ baryon signal has been measured from the reconstruction of the decay channels $\Lambda_c^+ \rightarrow pK_s^0$ ($K_s^0 \rightarrow \pi^+\pi^-$) and $\Lambda_c^+ \rightarrow pK^-\pi^+$. The weighted average of the results is compared to predictions based on FONLL for the beauty-hadron cross section in combination with PYTHIA 8 for the description of the $H_b \rightarrow \Lambda_c^+ + X$ decay kinematics. For these predictions, the beauty-quark fragmentation fraction of Λ_b^+ baryons measured by the LHCb Collaboration [18] and the fragmentation fractions of B^+ , B^0 and B_s^0 [5] for e^+e^- collisions were used. The production cross section is described by the model calculations for $p_T > 4$ GeV/c.

The p_T -dependent cross-section ratio for non-prompt Λ_c^+ baryons and non-prompt D^0 mesons is shown in Fig. 4 (right). Model calculations significantly underestimate the b-baryon production relative to the b-meson production for $p_T < 4$ GeV/c. In particular, the b-baryon production is enhanced with respect to model predictions that use $f(b \rightarrow \Lambda_b^+)$ from e^+e^- collisions or implement the branching ratio $\Lambda_b^+ \rightarrow \Lambda_c^+ + X$ as reported in [5]. This deviation might indicate different hadronisation mechanisms being at work in pp and e^+e^- collisions and that further not-yet measured beauty-hadron decays can contribute to the observed results.

The spin alignment of the vector meson D^{*+} with respect to the helicity axis has been studied by measuring the diagonal spin density matrix element ρ_{00} for prompt and non-prompt D^{*+} mesons via the reconstruction of the $D^{*+} \rightarrow D^0\pi^+$ ($D^0 \rightarrow K^-\pi^+$) decay channel together with its charge conjugate. The element ρ_{00} has been deduced from the angular distribution [19]

$$\frac{dN}{d\cos\theta^*} = N_0 \left[(1 - \rho_{00}) + (3\rho_{00} - 1) \cos^2\theta^* \right], \quad (1)$$

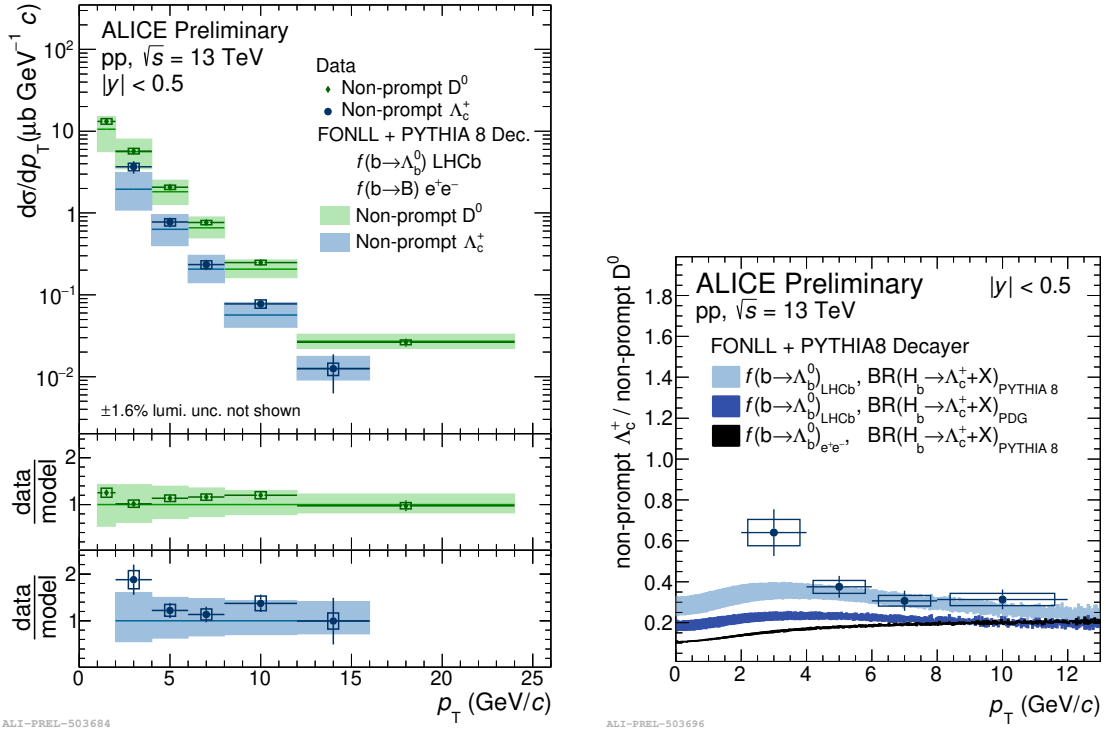


Figure 4: Measurement results of the cross section of non-prompt D^0 mesons and non-prompt Λ_c^+ baryons for pp collisions at $\sqrt{s} = 13$ TeV in comparison to predictions by FONLL and PYTHIA 8. The model calculations are tuned to measurements in Ref. [5, 18]. See text for more details. Left: the p_T -differential cross sections. Right: the ratio of the cross section for non-prompt Λ_c^+ baryons to non-prompt D^0 mesons.

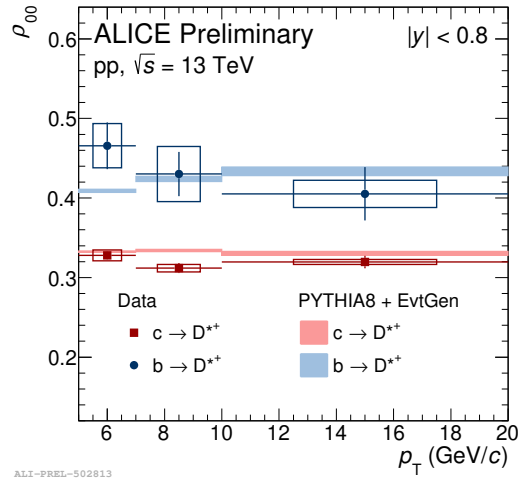


Figure 5: The element ρ_{00} of the spin density matrix for prompt and non-prompt D^{**} mesons as a function of p_T for pp collisions at $\sqrt{s} = 13$ TeV. The data are compared to predictions by PYTHIA 8 and EvtGen [20].

where N_0 is a normalisation constant and θ^* is the angle between the momentum direction of the D^0 (in the rest frame of the D^{*+}) and the helicity axis of the D^{*+} .

For prompt D^{*+} mesons, the measured element ρ_{00} is compatible with $1/3$ and thus with no polarisation of prompt D^{*+} mesons, as it can be seen in Fig. 5. On the other hand, the element ρ_{00} for non-prompt D^{*+} mesons is about 0.4 as expected for the decay of pseudo-scalar B mesons into vector mesons. Both measurements are consistent with predictions by PYTHIA 8 in combination with the EvtGen [20] decay package.

In conclusion, measurements for beauty-decay electrons, beauty jets, and non-prompt charm hadrons by the ALICE Collaboration have been presented for pp collisions at $\sqrt{s} = 13$ TeV. The main findings can be summarised as follows:

- the production of beauty electrons is described by pQCD calculations;
- the ratio of the cross section of non-prompt Λ_c^+ baryons to non-prompt D^0 mesons is well described for $p_T > 4$ GeV/c if the fragmentation fractions $f(b \rightarrow \Lambda_b^+)$ measured by LHCb are used instead of those from e^+e^- measurements;
- the non-prompt D-meson fraction exhibits no significant multiplicity dependence;
- prompt D^{*+} mesons are observed to be unpolarised. Non-prompt D^{*+} mesons show significant spin alignment, due to the helicity conservation in beauty-meson decays.

References

- [1] ALICE Collaboration, *JHEP* 05 (2021) 220.
- [2] ALICE Collaboration, *JHEP* 03 (2022) 190.
- [3] ALICE Collaboration, [arXiv:2202.00815](https://arxiv.org/abs/2202.00815) [nucl-ex]
- [4] Yang-guang Yang et al., *Phys. Rev. C* 97 (2018) 034917.
- [5] P. A. Zyla et al. (Particle Data Group), *Prog. Theor. Exp. Phys.* (2020) 083C01.
- [6] ALICE Collaboration, *JINST* 3 (2008) S08002.
- [7] ALICE Collaboration, *Phys. Lett. B* 721 (2013) 13-23.
- [8] ALICE Collaboration, *Phys. Lett. B* 738 (2014) 97-108.
- [9] M. Cacciari, M. Greco and P. Nason, *JHEP* 05 (1998) 007
M. Cacciari, S. Frixione and P. Nason, *JHEP* 03 (2001) 006.
- [10] Iván Schmidt and Marat Siddikov, *Phys. Rev. D* 101 (2020) 094020.
- [11] Peter Skands, Stefano Carrazza and Juan Rojo, *Eur. Phys. J. C* 74 (2014) 3024.
- [12] J. R. Christiansen and P. Z. Skands *JHEP* 08 (2015) 003.
- [13] C. Bierlich et al., *JHEP* 03 (2015) 148.
- [14] T. Sjöstrand, S. Mrenna and P. Skands, *JHEP* 05 (2006) 026
C. Bierlich et al., [arXiv:2203.11601](https://arxiv.org/abs/2203.11601) [hep-ph].
- [15] ALICE Collaboration, ALICE-PUBLIC-2016-005.
- [16] ALICE Collaboration, ALICE-PUBLIC-2021-005.
- [17] ALICE Collaboration, *Eur. Phys. J. C* 82 (2022) 6, 514.
- [18] LHCb Collaboration, *Phys. Rev. D* 100 (2019) 031102.
- [19] K. Schilling, P. Seyboth, and G. E. Wolf, *Nucl. Phys. B* 15 (1970) 397–412.
- [20] D. Lange, *Nucl. Instrum. Meth. A* 462 (2001) 152-155.